Alanine-Scanning Mutagenesis Reveals a Cytosine Deaminase Mutant with Altered Substrate Preference†

Sheri D. Mahan,‡ Greg C. Ireton,§ Barry L. Stoddard,§ and Margaret E. Black*,‡

Department of Pharmaceutical Sciences and the School of Molecular Biosciences, PO Box 646534, Washington State University, Pullman, Washington 99164-6534, and Fred Hutchinson Cancer Research Center, and the Graduate Program in Molecular and Cell Biology, University of Washington, 1100 Fairview Avenue N. A3-023, Seattle, Washington 98109

Received February 6, 2004; Revised Manuscript Received May 12, 2004

ABSTRACT: Suicide gene therapy of cancer is a method whereby cancerous tumors can be selectively eradicated while sparing damage to normal tissue. This is accomplished by delivering a gene, encoding an enzyme capable of specifically converting a nontoxic prodrug into a cytotoxin, to cancer cells followed by prodrug administration. The *Escherichia coli* gene, *cod*A, encodes cytosine deaminase and is introduced into cancer cells followed by administration of the prodrug 5-fluorocytosine (5-FC). Cytosine deaminase converts 5-FC into cytotoxic 5-fluorouracil, which leads to tumor-cell eradication. One limitation of this enzyme/prodrug combination is that 5-FC is a poor substrate for bacterial cytosine deaminase. The crystal structure of bacterial cytosine deaminase (bCD) reveals that a loop structure in the active site pocket of wild-type bCD comprising residues 310−320 undergoes a conformational change upon cytosine binding, making several contacts to the pyrimidine ring. Alanine-scanning mutagenesis was used to investigate the structure−function relationship of amino acid residues within this region, especially with regard to substrate specificity. Using an *E. coli* genetic complementation system, seven active mutants were identified (F310A, G311A, H312A, D314A, V315A, F316A, and P318A). Further characterization of these mutants reveals that mutant F316A is 14-fold more efficient than the wild-type at deaminating cytosine to uracil. The mutant D314A enzyme demonstrates a dramatic decrease in cytosine activity (17-fold) as well as a slight increase in activity toward 5-FC (2-fold), indicating that mutant D314A prefers the prodrug over cytosine by almost 20-fold, suggesting that it may be a superior suicide gene.

Suicide gene therapy of cancer is an appealing alternative to standard methods of chemotherapy because most chemotherapeutic agents lack tumor specificity. Classic chemotherapeutic agents are often unable to distinguish between tumor and normal dividing cells resulting in indiscriminate toxic effects. In contrast, suicide gene therapy allows for specific targeting of the tumor while preventing damage to normal cells. This is accomplished by introducing a gene encoding a prodrug-activating enzyme into cancer cells. While delivery systems have not been fully optimized, delivery of the gene is typically done using either a viral vector (retrovirus or adenovirus) or by other nonviral means (liposomes) (*1*−*3*). Once the gene is delivered into the cancer cell, a nontoxic prodrug is administered. The enzyme converts the nontoxic prodrug into its active and lethal form resulting in cancer cell death. *Escherichia coli* or bacterial cytosine deaminase (bCD)[1] is responsible for the activation of the nontoxic prodrug 5-fluorocytosine (5-FC) to its toxic form, 5-fluorouracil (5-FU) (*4*−*8*). The absence of an endogenous cytosine deaminase in mammalian cells provides for deamination of 5-FC only in cells that express bCD. This is followed by the conversion of 5-FU into its deoxyribonucleoside, fluorodeoxyuridine (FUdR) by thymidine phosphorylase. Upon phosphorylation of FUdR by endogenous thymidine kinase, thymidylate synthase is irreversibly inhibited by the product, 5FdUMP, thereby preventing dTTP formation and ultimately leading to inhibition of DNA synthesis.

One advantage of using the bCD/5-FC enzyme/prodrug combination is the phenomenon known as the bystander effect, defined as the killing of untransfected cells neighboring those cells transfected with the suicide gene (*9*). This type of killing has been described extensively with regard to the herpes simplex virus-1 thymidine kinase and ganciclovir enzyme/prodrug combination and occurs primarily by the transfer of toxic antimetabolites through gap junctions (*10*−*12*). Unlike phosphorylated ganciclovir, 5-FU is a small, uncharged molecule that can pass freely in and out of the cell by diffusion. As a consequence, cell−cell contact is not required for the bystander effect with bCD/5-FC, an advantage for those cell types with limited gap junctions (*13*).

The recently determined crystal structure of bacterial cytosine deaminase made it possible for us to identify active-site residues and select target regions for mutagenesis studies (*14*). For this study, residues 310−320 were chosen for alanine-scanning mutagenesis because this region has been

† This work was supported by National Institutes of Health Grants CA85939 (to M.E.B.), GM49857 (to B.L.S.), and CA97328 (to B.L.S. and M.E.B.).

* To whom correspondence should be addressed: Department of Pharmaceutical Sciences, PO Box 646534, Washington State University, Pullman, WA 99164-6534. Phone: (509) 335-6265. Fax: (509) 335-5902. E-mail: blackm@mail.wsu.edu.

‡ Washington State University.

§ University of Washington.

[1] Abbreviations: bCD, bacterial cytosine deaminase; 5-FC, 5-fluorocytosine; 5-FU, 5-fluorouracil.

10.1021/bi049720z CCC: $27.50
Published on Web 06/23/2004

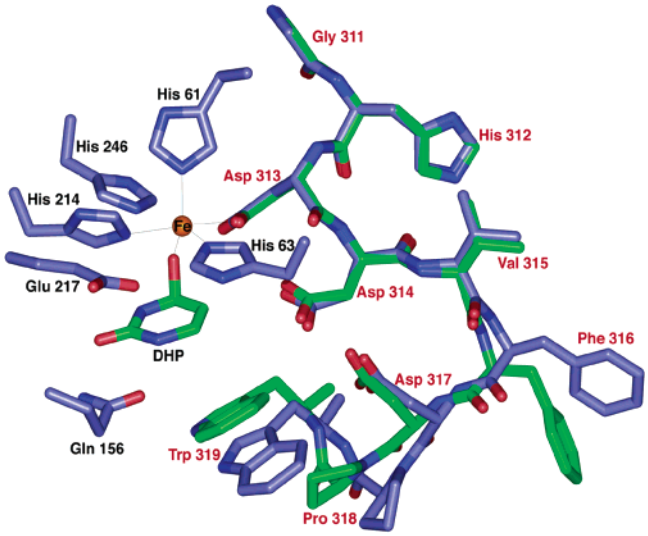

FIGURE 1: Active site residues of bCD. Residues in blue reflect the unbound enzyme, and residues in green reflect the conformational change upon substrate binding. DHP = dihydroxy pyrimidine (transition state analog). As seen in the model, there is a shift in residues 313−320 upon substrate binding. The four histidine residues H61, H63, H214, and H246 coordinate the iron ion. Residues F310 and Y320 are not shown.

shown to undergo a conformational change upon substrate binding and contains several amino acids in direct contact with the substrate (Figure 1). The goal of performing alanine-scanning mutagenesis is to investigate the role of these 11 amino acids and their importance to the structure−function relationship of the enzyme, especially with respect to substrate specificity. This will assist in optimization of the enzyme/prodrug interactions and may be valuable for the establishment of low dose treatments and enhancing the overall efficiency of this promising approach to cancer therapy.

MATERIALS AND METHODS

Materials. Oligonucleotides used for site-directed mutagenesis and DNA sequencing were purchased from Operon Technologies (San Pablo, CA). Restriction endonucleases used for screening alanine mutants were purchased from New England Biolabs (Beverly, MA). Nickel-affinity chromatography agarose (Ni-NTA Agarose) used to purify bCD enzymes was purchased from Qiagen (Valencia, CA). Protein purification, enzyme assay reagents, and other chemicals were purchased from Sigma (St. Louis, MO), unless otherwise noted.

Bacterial Strains. The cytosine deaminase deficient *E. coli* strain GIA39 (*thr*$^-$ *dad*B3 *fhu*A21 *cod*A1 *lac*Y1 *tsx*-95 *gln*V44(AS) λ^-*pyr*F101 *his*-108 *arg*G6 *ilv*A634 *thi*-1 *deo*C1 *glt*-15) was obtained from the *E. coli* Genetic Stock Center (CGSC 5594). *E. coli* GIA39 was lysogenized with DE3 according to the directions of the manufacturer (Novagen, Madison, WI). The derived strain, GIA39(DE3), was used in genetic complementation assays for cytosine deaminase activity. *E. coli* strain NM522 [F′ *lac*I^{q}Δ(*lac*Z)-M15*pro*A$^+$B$^+$/*sup*E *thi*Δ(*lac-pro*AB)Δ(*hsd*MS-*mcr*B)5($r_k^-m_k^-$McrBC$^-$)] was used as a recipient for certain cloning procedures. *E. coli* strain CJ236 (F$^+$LAM$^-$ *ung*-1 *rel*A1 *dut*-1 *spo*T1 *thi*-1) was used to produce single-stranded DNA for site-directed mutagenesis procedures. *E. coli* BL21(DE3) *tdk*$^-$ [F$^-$*omp*T[*lon*] *hsd*S_b ($r_B^-m_B^-$) *gal dcm met* (DE3)] was used for expression of the wild-type and mutant bCD proteins.

Vector. Construction of the pETHT vector is described by Brady et al. (*15*) and served as the backbone for the construction of pETHT:bCD. The 1.6-kb *Nco*I/*Hin*DIII fragment of bCD was cloned into pETHT (Novagen). An amino-terminal 6-His tag was used to aid in protein purification.

Site-Directed Mutagenesis of bCD. The expression vector, pETHT:bCD, was used to transform the *dut*$^-$*ung*$^-$ *E. coli* strain CJ236 for single-stranded DNA isolation. Single-stranded pETHT:bCD was used as a template for Kunkel-based site-directed mutagenesis (*16*). A total of 11 individual oligonucleotides containing the alanine mutation at the target amino acid and a silent mutation to introduce a restriction site for screening purposes were synthesized by Operon Technologies (San Pablo, CA). The mutagenic primers are designated by oligonucleotide name, position, and sequence (mutated nucleotides in bold), and new restriction site are listed below: MB293, F310A, 5′-ATCATCGTGGCCA**GC**GC-AG-3′, [*Msc*I]; MB294, G311A, 5′-GAAGACGTCATCGTG-**AG**CAAAGCAG-3′, [*Aat*II]; MB295, H312A, 5′-GAAGAC-GTCATCG**GC**ACCAAAG-3′, [*Aat*II]; MB296, D313A, 5′-GACATCA**G**CGTGGCCAAAG-3′, [*Msc*I]; MB292, D314A, 5′-GAAGAC**CG**CATCGTGGCCAAAC-3′, [*Msc*I]; MB297, V315A, 5′-GAAG**G**CATCATCGTGGCCAAAG-3′, [*Msc*I]; MB298, F316A, 5′-GATACCACGGATC**CGC**GACAT-CATCG-3′, [*Bam*HI]; MB299, D317A, 5′-GCGGGTAC-CACGGA**G**CGAAG-3′, [*Kpn*I]; MB308, P318A, 5′-GCGGG-TACCACG**C**ATCGAAG-3′, [*Kpn*I]; MB301, W319A, 5′-GCATATTCGCGGTACCCAGCGCATAC**GC**CGGATCG-3′, [*Kpn*I]; and MB302, Y320A, 5′-GCATATTCGCGG-TACCCAGCGGA**GC**CCACG-3′, [*Kpn*I]. After restriction enzyme verification, DNA-sequencing analysis performed at the core sequencing facility at Washington State University was used to confirm the presence of the altered sequence.

Primary Selection. Competent *E. coli* GIA39(DE3) (*cod*A deficient) cells were transformed with each bCD alanine mutant by electroporation. The transformants were initially plated on 2 × YT + carb^{50} plates and incubated at 37 °C overnight. Single clones were then picked and streaked for isolation onto control 2 × YT + carb^{50} and M9 uracil-containing plates. To determine complementation of enzyme activity (functionality), transformants were also streaked for isolation on cytosine-containing plates. The cytosine concentration in the selection medium ranged from 120 to 720 μM cytosine. The 2 × YT + carb^{50} plates were incubated at 37 °C overnight. The uracil and cytosine plates were incubated at 37 °C for 36 h. Positive selection was based on the genetic complementation of a functional bCD mutant transformed into the GIA39(DE3) *cod*A$^-$ strain. The CD selection uracil medium contained 0.36 g of yeast synthetic dropout without leucine, 50 mL of 10× M9 salts (15 g of KH_2PO_4, 33.9 g of anhydrous Na_2HPO_4, 2.5 g of NaCl, and 5.0 g of NH_4Cl for a total volume of 500 mL), 1 mM $MgSO_4$, 2.5 mL of 20% glucose, 0.1 mM $CaCl_2$, 1 mL of 2% leucine, 7.5 g of Bactoagar, and 50 μg/mL carbenicillin for a total volume of 500 mL. The CD selection cytosine medium contained 0.96 g of yeast synthetic dropout without uracil, 50 mL of 10× M9 salts, 1 mM $MgSO_4$, 2.5 mL of 20% glucose, 0.1 mM $CaCl_2$, 0.0267 mg/mL cytosine, 7.5 g of Bactoagar, and 50 μg/mL carbenicillin for a total volume of 500 mL.

Minimal	Uracil	Cytosine	5-FC (C + U)
wild-type	+	+	-
*cod*A, *pyr*F	+	-	+
*cod*A, *pyr*F + bCD	+	+	-
*cod*A	+	+	+
*pyr*F	+	+	-

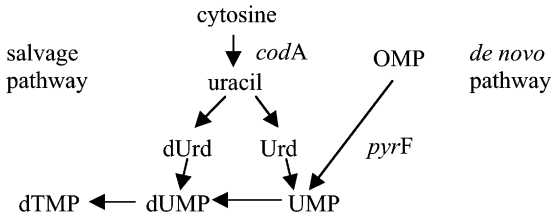

FIGURE 2: Genetic complementation for CD selection and 5-FC screening. Growth patterns of *E. coli* strains on minimal selection plates containing uracil, cytosine, or 5-FC with both pyrimidine sources. *Cod*A, cytosine deaminase-deficient *E. coli*; *pyr*F, OMP-decarboxylase-deficient *E. coli*; wild-type, *E. coli* with functional *cod*A and *pyr*F gene products; *cod*A *pyr*F, *E. coli* strain GIA39-(DE3); *cod*A *pyr*F + bCD, *E. coli* strain GIA39(DE3) containing pETHT:bCD. + = growth, and − = no growth. In the presence of uracil as a sole pyrimidine source, all strains will grow on minimal plates. When cytosine is the sole pyrimidine source, only cells containing a functional cytosine deaminase enzyme will grow. In the presence of 5-FC, cytosine, and uracil, only cells lacking a functional cytosine deaminase will be viable. The presence of bCD causes the conversion of 5-FC to 5-FU and results in cell death.

Secondary Selection. Alanine mutants found to complement bCD activity by positive genetic complementation were subjected to secondary selection to determine the sensitivity to the prodrug, 5-FC. Secondary selection media contained 5-FC concentrations ranging from 1 to 100 μg/mL (1, 2, 5, 10, 15, 20, 25, 50, and 100 μg/mL 5-FC). The 5-FC selection media contained 0.96 g of yeast synthetic dropout without uracil, 50 mL of 10× M9 salts, 1 mM $MgSO_4$, 2.5 mL of 20% glucose, 0.1 mM $CaCl_2$, 0.0267 mg/mL cytosine, 5−100 μg/mL 5-FC, and 50 μg/mL carbenicillin for a total volume of 500 mL.

When the GIA39(DE3) *E. coli* strain is used, the absence of a functional bCD makes the *cod*A-deficient strain insensitive to 5-FC. Therefore, 5-FC does not kill the cells, and growth occurs. However, if a functional bCD is present when 5-FC is added to cytosine-containing minimal plates, it is converted to 5-FU by the action of bCD and the cells are killed (Figure 2). Figure 2 shows the inclusion of uracil in addition to cytosine in the 5-FC selection plates. Uracil was used only to establish the negative selection and is not included in the experiments described here.

Expression and Purification of Wild-type and Mutant bCDs. Wild-type bCD and alanine mutant enzymes were expressed in the *E. coli* strain BL21(DE3) *tdk*$^-$. A 1 L culture of M9ZB medium [10 g of Bacto tryptone, 5 g of NaCl, diluted to 889 mL with water and then 100 mL of 10× M9 salts (30 g of KH_2PO_4, 67.8 g of Na_2HPO_4, 5 g of NaCl, and 10 g of NH_4Cl per liter), 1 mL of 1 M $MgSO_4$, 100 μL of 1 M $CaCl_2$, and 10 mL of 20% glucose added per liter] containing carbenicillin at 50 μg/mL was inoculated with 5 mL of M9ZB + carb^{50} starter culture and grown overnight at 30 °C. The cells were harvested at 4000*g* for 20 min at 4 °C, and the cell pellet was frozen at −20 °C overnight. Cleared lysates were prepared by thawing the cells for 15 min on ice and then resuspending the pellet in 2−5 mL/g wet weight of lysis buffer [50 mM NaH_2PO_4, 300 mM NaCl, and 10 mM imidazole at pH 8.0 (Calbiochem, La Jolla, CA)]. Lysozyme (1 mg/mL) was added to the resuspension, mixed, and incubated on ice. After incubation for 30 min, the cells were sonicated on ice (10 s pulses with 10 s pauses between bursts). The lysed cells were centrifuged at 10000*g* for 20−30 min at 4 °C. The cleared lysate was removed, passed through a 0.2 μm filter, and stored at −20 °C until purification.

The wild-type and alanine mutant enzymes were purified by nickel-affinity chromatography using Ni-NTA Agarose resin purchased from Qiagen (San Pablo, CA). Briefly, 4 mL of filtered cleared lysate was added to 1 mL of resin (50% Ni-NTA slurry) and allowed to mix on a rotating shaker for 1 h at 4 °C. The lysate/resin was batch-loaded into the column, and the flow-through was collected. The column was washed three separate times with 8 mL of wash buffer (50 mM NaH_2PO_4, 600 mM NaCl, and 20 mM imidazole at pH 8.0), and the three fractions were collected. The purified protein was eluted in four fractions with 0.5 mL of elution buffer (50 mM NaH_2PO_4, 300 mM NaCl, and 250 mM imidazole at pH 8.0). Aliquots of the cleared lysate, flow-through, three wash fractions, and four elution fractions were saved, and the efficiency of the purification was analyzed by sodium dodecyl sulfate−polyacrylaminde gel electrophoresis (SDS−PAGE).

For each purified protein, elution fractions were pooled and dialyzed in dialysis buffer (50 mM NaCl and 50 mM Tris at pH 7.5) at 4 °C. After dialysis, the samples were collected and stored at −20 °C. Protein concentrations for both the wild-type and all alanine mutants were determined using a bicinchoninic acid protein assay kit (Pierce, Rockford, IL) according to the instructions of the manufacturer. Purified proteins were subjected to SDS−PAGE, and the concentrations were found to correspond to known protein standards.

Enzyme Assays with Cytosine. Enzyme assays were performed as described by Ipata and Cercignani (*17*). Kinetic values for the wild-type and alanine mutants were obtained by measuring the change in absorbance over time using a spectrophotometer-based assay (Pharmacia Biotech Ultrospec 2000). A stock of 10−20 mM cytosine was made in 50 mM Tris-HCl at pH 7.5. Once optimal assay conditions were determined, the assays were completed for the wild-type and each of the seven functional mutants as follows: a zero time point was taken at the peak absorbance for cytosine (OD_{286}). The absorbance of the enzyme was also taken at OD_{286}. A cytosine concentration twice the desired concentration was diluted 1:1 with the enzyme to yield the desired cytosine concentration. OD_{286} readings were taken immediately upon mixing every 10 s for a total of 6.5 min (390 s). This was repeated using the same amount of enzyme for every cytosine concentration within the optimal range. Double reciprocal plots were used to determine K_m values for each mutant and wild-type bCD enzyme. The turnover number ($k_{cat} = V_{max}/[E]$, where $[E]$ is the total enzyme concentration) was also determined for each mutant and wild-type bCD. Assays were repeated 5−7 times.

Enzyme Assays with 5-FC. Kinetic values for the wild-type and D314A and F316A mutants were obtained using a protocol similar to that adapted from Hayden et al. (*18*). A stock of 30 mM 5-FC was made in 50 mM Tris-HCl at pH

Table 1: Growth Patterns of Wild-type and Alanine Mutants for Primary and Secondary Selection[a]

clone	complement bCD activity[b]	5-FC (μg/mL)
pETHT:bCD	+	20
pETHT	−	
F310A	+	20
G311A	+	20
H312A	+	20
D313A	−	
D314A	+	2
V315A	+	20
F316A	+	20
D317A	−	
P318A	+	20
W319A	−	
Y320A	−	

[a] The lowest concentration of 5-FC that each functional mutant is sensitive to is listed. [b] + = growth, and − = no growth.

7.5. Once optimal assay conditions were determined, assays were completed for the wild-type and D314A mutant. A 1 mL reaction was prepared using the desired concentration of 5-FC, enzyme, and 50 mM Tris-HCl at pH 7.5. The enzyme/substrate reaction proceeded at 37 °C for 15 min. Aliquots (50 μL) of the reaction were taken every 90 s and quenched in 0.1 N HCl. Readings were then taken at the peak absorbance for 5-FC (OD_{290}) and for 5-FU (OD_{255}). The following equations were used to determine both 5-FC and 5-FU drug concentrations (in millimolar): [5-FC] = $0.119A_{290} - 0.025A_{255}$ and [5-FU] = $0.105A_{255} - 0.049A_{290}$. Plots were made as described above. Assays were repeated 5−8 times.

RESULTS AND DISCUSSION

Complementation of Cytosine Deaminase Activity. For primary selection experiments, the 11 alanine mutants were used to transform the cytosine deaminase-deficient GIA39-(DE3) *E. coli* strain to assess bCD activity. Cells expressing a functional bCD grow on both uracil- and cytosine-containing plates, whereas cells that lack bCD or do not express a functional bCD will grow only on the nonselective uracil-containing plate (Figure 2). More specifically, this particular *E. coli* strain is deficient in both cytosine deaminase (*cod*A) and OMP decarboxylase (*pyr*F) and is unable to grow if cytosine is the sole pyrimidine source. When the *cod*A$^-$ *pyr*F$^-$ strain GIA39(DE3) expresses a plasmid-borne gene encoding a functional cytosine deaminase, cytosine can serve as the sole pyrimidine source. The presence of growth on plates where cytosine is the sole pyrimidine source indicates those mutants complement bCD activity or are functional. On the basis of the absence of growth on minimal plates containing cytosine, mutants are designated as non-functional.

We have established that *E. coli* GIA39(DE3) harboring the wild-type vector, pETHT:bCD, grows on minimal plates containing a cytosine concentration of 240 μM. As seen in Table 1, cells transformed with the positive control, wild-type pETHT:bCD, grew on cytosine plates, whereas the negative control, pETHT, that does not encode a functional bCD was not viable. Cells transformed with mutants F310A, G311A, H312A, D314A, V315A, F316A, and P318A also grew on cytosine-containing plates and were scored as functional bCD mutants (Table 1).

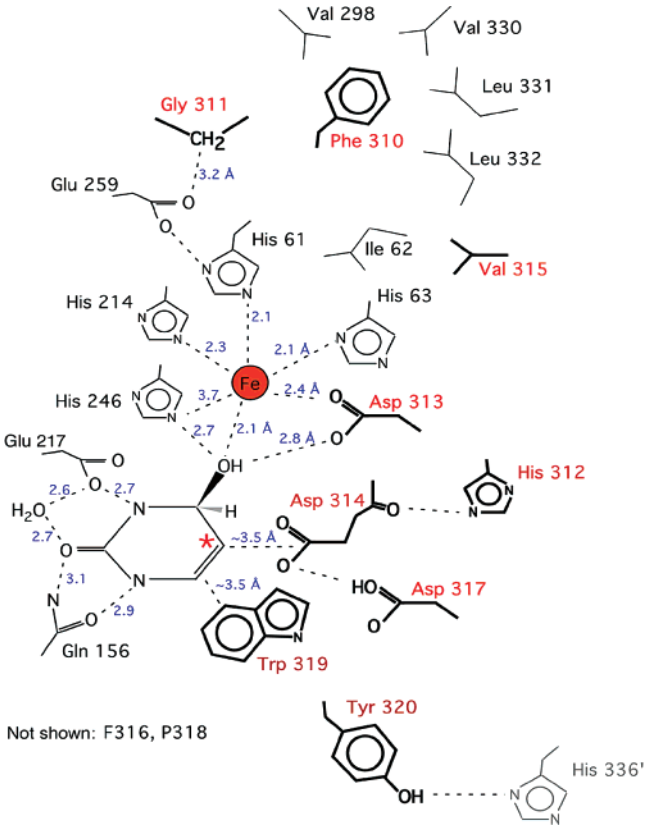

FIGURE 3: Enzyme active site with distances between bound, hydrated mechanism-based inhibitor (DHP), protein side chains, and the catalytic iron. Residues F316 and P318 are not shown.

Of the 11 alanine mutants generated, 7 complemented the cytosine deaminase-deficient *E. coli* (Table 1), while the remaining 4 (D313A, D317A, W319A, and Y320A) failed to complement the cytosine deaminase-deficient *E. coli* in the presence of cytosine (Table 1). The lack of activity by the D313A mutant is not entirely surprising because the crystal structure of bCD revealed that the D313 side chain is involved in coordinating the metal ion through electrostatic interactions and is also involved in substrate binding (Figure 3). In addition, residue D313 cooperates in the catalytic reaction by participating in proton transfer, acting as a general base. Residue D317 protrudes into the active site and is involved in hydrogen bonding interactions to T66 Oγ, D314 Oδ2, and the backbone N of Y320 and therefore may stabilize structural elements of the enzyme active site. Residue W319 directly stacks against the aromatic face of the cytosine substrate and appears to play an important role in substrate binding as well as in promoting a substrate-induced conformational change leading to active site closure (*14*). Y320 is located at the interface between the strand-swapped dimers within the hexameric bCD structure. The tyrosine hydroxyl of Y320 is hydrogen bonded with H336 of the adjacent monomer and coordinates a water molecule that also bonds to H332 across the dimer interface. Truncation of this residue to alanine likely destablizes the dimer interface leading to a loss of structural integrity and enzyme inactivation (Figures 1 and 3). The lack of ability to complement GIA39(DE3) shown by these mutants suggests that these residues are important to the structure and/or function of the enzyme. Because these four mutants fail to

Table 2: (Cytosine) Kinetic Values for the Nickel-Affinity-Purified Wild-type and Alanine Mutants Were Obtained Using a Spectrophotometer-Based Assay Adapted from Ipata and Cercignani (*17*)

enzyme	bCD (wild-type)	F310A	G311A	H312A	D314A	V315A	F316A	P318A
K_m (mM)	0.2 ± 0.09	ND[a]	ND	0.7 ± 0.07	2.2 ± 0.12	ND	0.2 ± 0.12	0.8 ± 0.3
k_{cat} (sec^{-1})[b]	165 ± 35	ND	ND	189 ± 110	104 ± 1.3	ND	2286 ± 816	1030 ± 38
k_{cat}/K_m (sec^{-1} mM^{-1})	825	ND	ND	269.6	47.4	ND	11 431	1288
relative to the wild-type	1	ND	ND	0.33	0.06	ND	13.9	1.6

[a] ND = not detectable. [b] $k_{cat} = V_{max}/[E]$, where $[E]$ is the total enzyme concentration.

complement bCD activity, they were not considered for further characterization.

Sensitivity of Cells Expressing Alanine Mutants to 5-FC. The seven alanine mutants found to complement bCD activity by positive genetic complementation were subjected to secondary selection to determine if there is an increased activity toward 5-FC relative to that of the wild-type (Table 1). At 5-FC concentrations of 20 μg/mL or less in the plate assay, cells expressing wild-type bCD are viable. Any mutants with an increased sensitivity/activity toward 5-FC compared to that of the wild-type will be unable to form colonies at 20 μg/mL 5-FC. Of the seven alanine mutants tested, only mutant D314A shows an increase in sensitivity to the prodrug with growth occurring at concentrations of 2 μg/mL or less of 5-FC (Table 1), a concentration 10-fold lower than that which allows wild-type bCD to grow. The increase in sensitivity indicates that mutant D314A may be better than wild-type bCD at converting the nontoxic prodrug into its toxic form.

Enzyme Assays (Cytosine). Wild-type bCD and the seven functional alanine mutants were purified to near homogeneity by nickel-affinity chromatography. The purified proteins were examined by SDS−PAGE and revealed a single prominent band that migrated at ~52 kDa. The purified protein was then quantified and used for enzyme assays. Enzyme assays using cytosine as the substrate were performed to evaluate the effects of the amino acid substitutions on the kinetic behavior of the wild-type bCD and seven alanine mutant enzymes. The following summary of the biochemical characterization of bCD constructs will begin with the wild-type enzyme followed by mutant enzymes in order of their relative catalytic efficiencies, beginning with those exhibiting activities below the detection limits of the assay to an activity greater than that of the wild-type.

Wild-type bCD. As shown in Table 2, the calculated K_m for wild-type bCD is 0.2 mM cytosine. The k_{cat} for wild-type bCD is 165 s^{-1}, and the efficiency of the wild-type enzyme for cytosine (k_{cat}/K_m) is 825 s^{-1} mM^{-1}. Kinetic data obtained for wild-type bCD are in agreement with values reported by Porter (*19*).

Mutants with Activity Below the Range of Assay Detection Limits (F310A, G311A, and V315A). The detection limit of the assay for K_m values is between 0.05 and 3.0 mM cytosine. Although they are capable of complementing a genetic cytosine deaminase deficiency, enzymatic activities for mutants F310A and G311A were not measurable at cytosine concentrations 8-fold lower to 15-fold higher than that used for wild-type bCD (Table 2). The lack of enzymatic activity may be due to protein instability and/or increased degradation as suggested by poor expression and low yields of purified protein. F310 sits in a buried pocket and is in van der Waals surface contact with numerous other hydrophobic residues: A274, P276, V298, V330, L331, G334, and L352, all within 3.6−4.0 Å from the phenylalanine ring. Truncation to alanine essentially leaves a cavity that may greatly destabilize the protein. The backbone α carbon for G311 is only 3.2 Å from side chain oxygens on E59 and N275. The change to alanine at 311 positions the side chain carbon under 1.9 Å from these residues that are involved in hydrogen bonding to H61 and H246. Disruption of either E59 or N275 because of the steric clash with G311A likely results in suboptimal metal coordination, substrate binding, and structural stability (Figure 3).

Mutant V315A also exhibits a lack of enzymatic activity at enzyme concentrations 70-fold lower to 2.1-fold greater and cytosine concentrations 13-fold lower to 30-fold greater than that used for wild-type bCD (Table 2). Unlike F310A and G311A, the expression, yield, and solution behavior of the purified protein was similar to that of the wild-type, implying that the protein is not significantly destabilized. A denaturation analysis of the enzyme at elevated temperatures, conducted by circular dichroism, indicated that the protein melting point (TM) is slightly reduced relative to that of the wild-type (approximately 75 versus 85 °C) but is still well above ambient temperatures used for enzyme assays (data not shown). The reason for the minor destabilization and reduced activity of V315A is not immediately clear. The side chain of V315 sits adjacent to H312 and I62. Disruption of van der Waals contacts (hydrophobic packing) could cause a shift that alters the position of either critical metal-binding residue H61 or H63, leading to enzyme inactivation (Figure 3).

Mutants with Reduced Activity (H312A and D314A). Both H312A and D314A are less efficient at deaminating cytosine to uracil relative to the wild-type but display measurable kinetic profiles (Table 2). Mutant H312A has a K_m of 0.7 mM for cytosine compared to the 0.2 mM K_m for the wild-type. The calculated k_{cat} value (189 s^{-1}) shows that this mutant has a similar reaction rate compared to that of the wild-type. A 3-fold decrease in k_{cat}/K_m for H312A relative to that of wild-type bCD indicates that this mutant is a less efficient enzyme. The Nϵ2 of H312 is hydrogen bonded to the backbone oxygen of D314. A possible consequence of truncating this residue to alanine is a perturbation of the peptide backbone and a subtle repositioning of residue 313 or 314, such that the substrate-binding interface is compromised.

The kinetic data for mutant D314A reveal that this mutant has an affinity for cytosine that is 11-fold lower than that of wild-type bCD (2.2 versus 0.2 mM) (Table 2). In addition, the rate of reaction is decreased relative to that of the wild-type. The decrease in both K_m and k_{cat} values results in a mutant that is 17-fold less efficient than that of the wild-type when using cytosine as the substrate. The decrease in

cytosine binding and turnover is likely due to the reduced van der Waals contact between residue 314 and the 5′ position of the pyrimidine ring, possibly causing increased conformational flexibility in the bCD active site pocket. Another predicted consequence of this mutation is a loss of hydrogen bonding to D313 and D317 that may also cause subtle realignment of the active site structural elements, most notably the loop region itself, residues 313−320, and the β1 strand of the $(\alpha\beta)_8$ barrel domain containing H61 and H63, which coordinate the metal ion (Figure 3).

Mutant with Similar Cytosine Activity (P318A). Mutant P318A is the only alanine mutant that has an overall activity similar to that of wild-type bCD (Table 2). The calculated K_m for this mutant is 4.0-fold higher (0.8 versus 0.2 mM) in comparison to that of the wild-type, indicating that mutant P318A has a lower binding affinity for cytosine than wild-type bCD. However, the calculated k_{cat} value is higher than that of the wild-type (6.2-fold), signifying an increased rate for utilizing cytosine. Mutant P318A is also more efficient than the wild-type when using cytosine, as indicated by the k_{cat}/K_m value. In other words, mutant P318A does not bind cytosine as strongly as the wild-type enzyme, but when it does bind, it converts cytosine to uracil efficiently. Overall, relative to the wild-type, mutant P318A has a similar cytosine specificity (1.6-fold relative specificity).

As shown in Figure 1, P318A is in a loop region of the active site that appears to undergo a conformational shift when the substrate is bound, leading to the lower affinity for cytosine. It is likely that the conformational change occurs more efficiently when the steric backbone constraints of the proline residue are eliminated, leading to an increase in the reaction rate, at the expense of some binding energy, by improving the kinetics of loop movement during the catalytic cycle.

Mutant with Increased Activity (F316A). Mutant F316A shows a K_m of 0.2 mM cytosine, similar to the K_m determined for the wild-type. Therefore, the F316A residue can be replaced with an alanine residue without causing an alteration in the affinity of the enzyme toward cytosine. However, the most interesting characteristic of mutant F316A is the 13.9-fold increase in the reaction rate (k_{cat}), which contributes to an overall increase in specificity (k_{cat}/K_m) of 13.9-fold, relative to that of the wild-type.

As shown in Figure 1, a conformational shift occurs mainly in the loop region of the active site of bCD. Residue F316 is located in the mobile loop and appears to undergo a large conformational shift upon substrate binding. When the smaller alanine residue is substituted for the aromatic phenylalanine at position 316, the shift may occur more easily, thereby facilitating catalysis by closing the active site more effectively. This allows for a more efficient catalysis of cytosine to uracil (13.9-fold). The position of the backbone at residue 316 does not affect substrate binding, because there is no change in K_m. As was hypothesized above for the P318A mutant, what is likely to be affected is the rate at which this mobile element (region 313−319) is able to open and close. For the F316 side chain to move, a hydrogen bond must be broken between the C-terminal R426 of the adjacent strand-swapped dimer and the backbone oxygen of A70 (at the hinge point for the larger domain movement involving residues 69−96). Both of these elements also have movements associated with enzyme catalysis. Truncation to alanine allows 316 to move without encountering a steric clash.

Table 3: (5-FC) Kinetic Values for the Wild-type, D314A, and F316A Mutants Were Obtained Using a Spectrophotometer-Based Assay Adapted from Hayden et al. (*18*)

enzyme	bCD (wild-type)	D314A	F316A
K_m (mM)	3.3 ± 1.4	2.8 ± 0.4	2.1 ± 0.25
k_{cat} (sec^{-1})[a]	75.6 ± 0.0	137.4 ± 0.0	74.3 ± 0.0
k_{cat}/K_m (sec^{-1} mM^{-1})	23.0	50.0	35.4
relative to the wild-type	1.00	2.18	1.54
$[k_{cat}/K_m$ (5-FC)]/ $[k_{cat}/K_m$ (cytosine)] + $[k_{cat}/K_m$ (5-FC)]	0.027	0.513	0.003

[a] $k_{cat} = V_{max}/[E]$, where $[E]$ is the total enzyme concentration.

Enzyme Assays (5-FC): Wild-type bCD and Mutant D314A. To further investigate the increased 5-FC sensitivity observed in the plate assay, the kinetic parameters for the *E. coli* expressing the wild-type and D314A mutant were determined. As shown in Table 3, the K_m for wild-type bCD is 3.3 mM 5-FC. The k_{cat} for wild-type bCD using 5-FC as the substrate is 75.6 s^{-1}, and the efficiency of the wild-type enzyme for 5-FC (k_{cat}/K_m) is 23 s^{-1} mM^{-1}. When 5-FC is used as the substrate, mutant D314A has a K_m of 2.8 mM. Relative to the wild-type, this K_m indicates that D314A has a similar affinity toward 5-FC. However, the rate at which D314A converts 5-FC to 5-FU is 1.8-fold higher. On the basis of K_m and k_{cat} data, the efficiency (k_{cat}/K_m) of mutant D314A for 5-FC is 2.18-fold greater than that of the wild-type.

While this 2.18-fold increase in activity for D314A is not significantly higher than that of the wild-type, this mutant enzyme does show an enhanced preference for the prodrug in *E. coli*. Because endogenous cytosine within the cell can compete with 5-FC for the active site, it is important to consider the ratio of specificity constants that the wild-type and mutant D314A have for both the prodrug and cytosine. When considering the relative specificity that the wild-type and D314A have for 5-FC and cytosine ($[k_{cat}/K_m$ (5-FC)]/ $[k_{cat}/K_m$ (cytosine)] + $[k_{cat}/K_m$ (5-FC)]), there is a 19-fold difference between the two enzymes (Table 3). This kinetic datum indicates that D314A prefers 5-FC over cytosine for its substrate. This preference is a result of mutant D314A having a cytosine activity that is greatly impaired rather than having a substantially improved 5-FC activity. The altered degree of competition between cytosine and 5-FC suggests that D314A is a better candidate than the wild-type for use in suicide gene therapy.

Figures 1 and 3 clearly show the side chain of residue 314 protruding into the active site of bCD. In the presence of a nonfluorinated cytosine substrate analogue, the measured distance from the side chain carboxylate oxygens of D314 to the 5′ carbon is approximately 3.5 Å. Modeling of a fluorinated substrate into this binding site leads to a prediction of electrostatic repulsion with the wild-type D314 side chain. Substitution of an alanine for the aspartic acid side chain is predicted to eliminate this repulsion with a 5′ fluorine substituent. This may lead to stabilization of the transition state, thus leading to the increase in efficiency displayed by mutant D314A.

In a separate study, error prone PCR was used to introduced mutations randomly throughout the entire bCD

open reading frame (20). Surprisingly, the mutant identified to confer the highest degree of sensitivity to 5-FC in the negative selection system contained only two amino acid substitutions, Q102R and D314G. Additional site-directed mutagenesis of these two sites led us to identify D314G as being solely responsible for the enhanced sensitivity. Such parallel results provide strong evidence for the significant role that D314 plays in substrate specificity and utilization.

Mutant F316A. The F316A kinetic values for cytosine indicate that the mutant is 14.5-fold more efficient at deaminating cytosine to uracil because of a 13.9-fold increase in k_{cat} (Table 2). Because this increased turnover rate may mask a concomitant increase in activity toward 5-FC in the plate assays, we examined the ability of F316A to deaminate 5-FC using enzyme assays. As shown in Table 3, F316A demonstrates a K_m of 2.1 mM 5-FC, indicating that this mutant has a slightly better binding affinity for the prodrug. However, the k_{cat} for this mutant is 74.3 s^{-1}, nearly identical to that of wild-type bCD. Thus, the efficiency (k_{cat}/K_m) of this mutant for converting 5-FC to 5-FU is only 1.54-fold higher than that of the wild-type. Interestingly, the increased turnover rate observed with cytosine is not observed when 5-FC is the substrate. The most likely explanation for this observation is that the rate-limiting step of the reaction is different for cytosine and 5-fluorocytosine substrates. For the wild-type enzyme, the movement of the enzyme active site loop during substrate binding and/or product release appears rate-limiting ($k_{cat} \sim 165$ s^{-1}) and that rate can be increased by mutating F316 in that loop to an alanine residue. In contrast, the rate-limiting step of deamination for 5-FC is slower ($k_{cat} \sim 74$ s^{-1}) and appears to involve the transition state of the deamination reaction step, so that the same F316A mutation in the mobile loop does not alter the turnover rate of the enzyme.

Enzyme Structure, Mechanism, and Substrate Specificity. Enzymes that catalyze the deamination of both cytosine and adenosine to uracil and inosine, respectively, are responsible for base salvage in prokaryotes and single-cell eukaryotes and for a variety of DNA- and RNA-editing processes. Recent structural studies have demonstrated that nucleoside deamination activities have evolved independently at least twice on two completely unique protein scaffolds (in one case, a classical α/β "TIM" barrel and, in the second case, a smaller amidohydrolase fold, first described for *E. coli* cytidine deaminase) (*14*, *21*, *22*). Variants of both structural enzyme types have been visualized that act specifically on cytosine or adenosine, on nucleobases or nucleosides, and on DNA or RNA. For both folds, conserved active site residues form the binding site of a catalytically essential metal (either a zinc or an iron) and contribute an equally essential glutamate residue that acts as a general base for proton transfer (*22*). Also, unique structural elaborations surrounding the catalytic core provide the side chains and structural elements that impart substrate specificities to individual enzymes. For members containing the amidohydrolase fold, most of these diverged side chains are presented to the active site by variable C-terminal peptides. In contrast, for the bCD α/β barrel enzyme described in this work, the majority of residues that participate in substrate recognition and specificity are found on a pair of mobile loops that guard the entrance to the barrel and the corresponding active site. In the crystal structure of bCD, these loops rotate inward upon binding of a mechanism-based inhibitor by up to 6 Å, leading to the formation of a large number of polar−nonpolar contacts to the pyrimidine ring (*14*). Residues 315−319 on one of these loops are presented to the region surrounding the 5′ position of the ring and contribute to specificity at that position.

The bCD enzyme catalyzes an essentially irreversible deamination of a cytosine nucleobase. The reaction proceeds by addition of a hydroxyl group to the cytosine substrate at the C4 position. Water is the source of the newly incorporated oxygen in the product, by addition of a metal bound activated solvent molecule. The reaction proceeds by a conformational change in the substrate molecule during the course of the nucleophilic attack, in which a tetrahedral transition state intermediate is formed because of the loss of aromaticity and transient protonation of the N3 pyrimidine nitrogen (*14*). Structural and kinetic analyses of the *E. coli* cytidine deaminase and the human adenosine deaminase indicate that maximizing the contact surface between the enzyme and substrate at this step of the reaction is advantageous for the enzymes to take full advantage of forces between catalytic groups and the transition state and to maximize both turnover rate and substrate specificity (*23*−*25*). The results of this study indicate that perturbation and mutation of the residue in immediate proximity to the 5′ pyrimidine position (D314) can preferentially shift the *in vivo* substrate flux for the enzyme toward 5-FC relative to cytosine, by destabilizing the natural (cytosine) enzyme−substrate complex and/or transition state complex (leading to a 10-fold increase in K_m) while displaying little effect on 5-FC binding. The effects of this mutation appear to be limited to the affinity of the enzyme for cytosine relative to 5-FC while, at the same time, causing only small, relatively insignificant alterations of the maximal turnover rate (k_{cat}), indicating that the D314A mutation does not cause a significant impairment in proton transfer, in the ability of the enzyme to activate the metal bound nucleophilic water or in the charge stabilization of the transition state.

In conclusion, the results reported here reveal that D314A is a superior candidate for suicide gene therapy. Its poor efficiency for cytosine in combination with a slight increase in efficiency for 5-FC suggests that competition for the active site within a cell between cytosine and 5-FC is reduced, a distinct advantage in a gene therapy setting. The ability of D314A to convert more 5-FC to 5-FU also suggests that it may be possible to administer less prodrug for a more-effective tumor ablation.

ACKNOWLEDGMENT

We would like to thank R. M. Blaese for his gift of bCD.

REFERENCES

1. Szala, S., Missol, E., Sochanik, A., and Strozyk, M. (1996) The use of cationic liposomes DC-CHOL/DOPE and DDAB/DOPE for direct transfer of *Escherichia coli* cytosine deaminase gene into growing melanoma tumors, *Gene Ther. 3*, 1026−1031.
2. Hlavaty, J., Hlubinova, K., and Altaner, C. (1999) Construction and testing of gene therapy retroviral vector expressing bacterial cytosine deaminase gene, *Neoplasma 46*, 267−276.
3. Wu, Q., Moyana, T., and Xiang, J. (2001) Cancer gene therapy by adenovirus-mediated gene transfer, *Curr. Gene Ther. 1*, 101−122.

4. Austin, E. A., and Huber, B. E. (1992) A first step in the development of gene therapy for colorectal carcinoma: Cloning, sequencing, and expression of *Escherichia coli* cytosine deaminase, *Mol. Pharmacol. 43*, 380−387.
5. Mullen, C. A., Kilstrup, M., and Blaese, R. M. (1992) Transfer of the bacterial gene for cytosine deaminase to mammalian cells confers lethal sensitivity to 5-fluorocytosine: A negative selection system, *Proc. Natl. Acad. Sci. U.S.A. 89*, 33−37.
6. Huber, B. E., Austin, E. A., Good, S. S., Knick, V. C., Tibbels, S., and Richards, C. A. (1993) *In vivo* antitumor activity of 5-fluorocytosine on human colorectal carcinoma cells genetically modified to express cytosine deaminase, *Cancer Res. 53*, 4619−4626.
7. Hirschowitz, E. A., Ohwada, A., Pascal, W. R., Russi, T. J., and Crystal, R. G. (1995) *In vivo* adenovirus-mediated gene transfer of the *Escherichia coli* cytosine deaminase gene to human colon carcinoma-derived tumors induces chemosensitivity to 5-fluorocytosine, *Hum. Gene Ther. 6*, 1055−1063.
8. Kievit, E., Bershad, E., Ng, E., Sethna, P., Dev, I., Lawrence, T. S., and Rehemtulla, A. (1999) Superiority of yeast over bacterial cytosine deaminase for enzyme/prodrug gene therapy in colon cancer xenografts, *Cancer Res. 59*, 1417−1421.
9. Moolten, F. L. (1986) Tumor chemosensitivity conferred by inserted herpes thymidine kinase genes: Paradigm for a prospective cancer control strategy, *Cancer Res. 46*, 5276−5281.
10. Bi, W. L., Parysek, L. M., Warnick, R., and Stambrook, P. J. (1993) *In vitro* evidence that metabolic cooperation is responsible for the bystander effect observed with HSV-tk retroviral gene therapy, *Hum. Gene Ther. 4*, 725−731.
11. Mesnil, M., Piccoli, C., Tiraby, G., Willecke, K., and Yamasaki, H. (1996) Bystander killing of cancer cells by herpes simplex virus thymidine kinase gene is mediated by connexins, *Proc. Natl. Acad. Sci. U.S.A. 93*, 1831−1835.
12. Duflot-Dancer, A., Piccoli, C., Rolland, A., Yamasaki, H., and Mesnil, M. (1998) Long-term connexin-mediated bystander effect in highly tumorigenic human cells *in vivo* in herpes simplex virus thymidine kinase/ganciclovir gene therapy, *Gene Ther. 5*, 1372−1378.
13. Domin, B. A., Mahony, W. B., and Zimmerman, T. P. (1993) Transport of 5-fluorouracil and uracil into human erythrocytes, *Biochem. Pharmacol. 46*, 503−510.
14. Ireton, G. C., McDermitt, G., Black, M. E., and Stoddard, B. L. (2002) The structure of *E. coli* cytosine deaminase at 1.5 Å resolution, *J. Mol. Bio. 315*, 687−697.
15. Brady, W. A., Kokoris, M. S., Fitzgibbon, M., and Black, M. E. (1996) Cloning, characterization, and modeling of mouse and human guanylate kinases, *J. Biol. Chem. 271*, 16734−16749.
16. Kunkel, T. A. (1985) Rapid and efficient site-specific mutagenesis without phenotypic selection, *Proc. Natl. Acad. Sci. U.S.A. 82*, 488−492.
17. Ipata, P. L., and Cercignani, G. (1978) Cytosine and cytidine deaminase from yeast, *Methods Enzymol. 51*, 395−400.
18. Hayden, M. S., Linsley, P. S., Wallace, A. R., Marquardt, H., and Kerr, D. E. (1998) Cloning, overexpression, and purification of cytosine deaminase from *Saccharomyces cerevisiae*, *Protein Expression Purif. 12*, 173−184.
19. Porter, D. J. T. (2000) *Escherichia coli* cytosine deaminase: The kinetics and thermodynamics for binding of cytosine to the apoenzyme and the Zn^{2+} holoenzyme and similar, *Biochim. Biophys. Acta 1476*, 239−252.
20. Mahan, S. D., Ireton, G. C., Knoeber, C., Stoddard, B. L., and Black, M. E. Random mutagenesis of *E. coli* cytosine deaminase for cancer gene therapy, manuscript submitted.
21. Betts, L., Xiang, S., Short, S. A., Wolfenden, R., and Carter, C. W., Jr. (1994) Cytidine deaminase. The 2.4-Å crystal structure of an enzyme: Transition-state analog complex, *J. Mol. Biol. 235*, 635−656.
22. Ireton, G. C., Black, M. E., and Stoddard, B. L. (2003) The 1.14-Å crystal structure of yeast cytosine deaminase: Evolution of nucleotide salvage enzymes and implications for genetic chemotherapy, *Structure 11*, 961−972.
23. Wilson, D. K., Rudolph, F. B., and Quiocho, F. A. (1991) Atomic structure of adenosine deaminase complexed with a transition-state analog: Understanding catalysis and immunodeficiency mutations, *Science 252*, 1278−1284.
24. Wang, Z., and Quiocho, F. A. (1998) Complexes of adenosine deaminase with two potent inhibitors: X-ray structures in four independent molecules at pH maximum activity, *Biochemistry 37*, 8314−8324.
25. Wilson, D. K., and Quiocho, F. A. (1993) A pre-transition-state mimic of an enzyme: X-ray structure of adenosine deaminase with bound 1-deazaadenosine and zinc-activated water, *Biochemistry 32*, 1689−1694.

BI049720Z